Chirality-dependent environmental effect in photoluminescence of single-walled carbon nanotubes

Yutaka Ohno,[1, *] Shinya Iwasaki,[1] Yoichi Murakami,[2] Shigeru
Kishimoto,[1] Shigeo Maruyama,[2] and Takashi Mizutani[1, †]

[1]*Department of Quantum Engineering, Nagoya University,*

Furo-cho, Chikusa-ku, Nagoya 464-8603, Japan

[2]*Department of Mechanical Engineering,*

The University of Tokyo, 7-3-1 Hongo,

Bunkyo-ku, Tokyo 133-8656, Japan

(Dated: June 4, 2006)

Abstract

The optical transition energies, E_{11} and E_{22}, of single-walled carbon nanotubes (SWNTs) suspended in air have been investigated for 20 species by photoluminescence and excitation spectroscopies. We have studied the environmental effects in photoluminescence by comparing our results with those for the SWNTs wrapped by sodium-dodecyl-sulfate (SDS), as reported by Weisman *et al.* The energy differences between air-suspended and SDS-wrapped SWNTs, $\Delta E_{ii} = E_{ii}^{\mathrm{air}} - E_{ii}^{\mathrm{SDS}}$, depends on the chiral vector (n,m), specifically on the chiral angle and type of SWNT (type-I or type-II). The ΔE_{11} and ΔE_{22} mostly blueshifted, with the exception of the ΔE_{22} of some type-II SWNTs (that have a small chiral angle), which redshifted. With an increase in the chiral angle, the ΔE_{11} increased in type-I SWNTs and decreased in type-II SWNTs. In contrast, the ΔE_{22} demonstrated opposite dependence on the chiral angle. The differences in ΔE_{11} and ΔE_{22} between type-I and type-II disappeared in the SWNTs with chiral angles close to 30° (near armchair). The (n,m) dependence of the environmental effect on the transition energies can be explained by the difference in the effective mass, which contributes to the energy of Coulomb interactions between carriers.

I. INTRODUCTION

The photoluminescence (PL) spectroscopy of single-walled carbon nanotubes (SWNTs) has received increasing attention, not only for assigning the chiral vector, (n,m), of the SWNTs[1-3] but also to study the physics of the one-dimensional excitons[4-7]. Following the report of O'Connell et al.[8], individual SWNTs encased in a micelle in a surfactant solution, such as sodium-dodecyl-sulfate (SDS), have been widely used to investigate the physics of PL in SWNTs.

Some groups have reported that the optical transition energies vary depending on the kind of surrounding materials used to individualize SWNTs[5,6,9-11]. This has been attributed to the *environmental effect*, produced by differences in the dielectric constants of the surfactants. The exciton binding energy in SWNTs depends on the matrix in which the SWNTs are placed, because the electric force lines contributing to the electron-hole interaction pass mainly through the matrix rather than through the inside of the SWNT[12,13]. The experimental results of PL and resonant Raman scattering have been reported for SWNTs in various environmental conditions in addition to SDS, for instance, DNA-wrapped SWNTs[6] and bundled SWNTs[10].

In particular, SWNTs suspended in air, which have been grown between pillars or over trench, are important for investigating the environmental effect because of the near-unit dielectric constant of the air[14-16]. Lefebvre et al. have measured E_{11} and E_{22} of SWNTs suspended in air between pillars by PL spectroscopy[15]. They described that air-suspended SWNTs and micelle-wrapped SWNTs give rise to broadly similar optical spectra, with subtle species-dependent differences. The emission and absorption energies of the seven species compared differed by 2 to 5%. The optical transition energies of the air-suspended SWNTs blueshifted by an average of 28 meV for E_{11} and 16 meV for E_{22} in 7 species, as compared to SDS-wrapped SWNTs[15]. These shifts depend weakly on the particular (n,m) and diameter of the SWNTs; however, a detailed understanding of the environmental effect is still lacking.

According to theoretical works, the exciton binding energy in SWNTs depends not only on the dielectric constant of the environment, but also on the diameter of the SWNT and the effective mass of carriers[12,13,17]. In the case of SWNTs, the effective mass strongly depends on the (n,m) because of the trigonal warping effect of the energy band near the K-point. This would lead to the expectation that the dielectric environmental effect also depends on (n,m).

In this experiment, we have investigated E_{11} and E_{22} for 20 species of air-suspended SWNTs grown on a quartz substrate with periodic grooves and having a sufficient energy resolution. The E_{11} and E_{22} have been compared to those of the SDS-wrapped SWNTs reported by Weisman $et\ al.$ Results show that the energy differences between the air-suspended and the SDS-wrapped SWNTs depend on (n,m), in particular, on the chiral angle and type of SWNT (type-I $[(2n + m) \bmod 3 = 1]$ or type-II $[(2n + m) \bmod 3 = 2]$).

II. EXPERIMENTAL

For this work, we used SWNTs suspended in air that had been grown on a quartz substrate with periodic grooves. The plan-view and bird-view SEM images are shown in Fig. 1. Both the period and depth of the grooves are 2 μm. The grooves were formed by photolithography, Al-metal evaporation and lift-off, and subsequent reactive-ion etching of the quartz with the Al mask. The SWNTs were grown by alcohol catalytic chemical vapor deposition at 750°C after deposition of Co and Mo catalysts by the dip coating method[18]. The SWNTs bridged over the groove during the growth and were well aligned perpendicular to the groove. The density of the SWNTs was about 10 μm^{-1}. Measurements of PL and PL excitation spectra were performed using a tunable continuous-wave Ti/Sapphire laser (700∼950 nm), a monochromator with a focal length of 25 cm, and a liquid N$_2$-cooled InGaAs photomultiplier tube (900∼1700 nm). The excitation wavelength was monitored by a laser wavelength meter. The energy resolution and accuracy in the present measurements are both ∼2 meV at the worst. The diameter of laser spot on the sample surface was about 1 mm, so that an ensemble of many SWNTs was detected. The spectral width measured in the present study was 20∼30 meV, which was not very different from the SDS-wrapped SWNTs. We have previously measured individual air-suspended SWNTs by micro-PL[16]. Their linewidths were as narrow as 8∼12 meV, but the peak energies scattered by ∼20 meV even in the same (n,m) SWNTs. Therefore, the broad spectral width of the present macro-PL measurement is attributed to the inhomogeneous broadening. Although we do not have an adequate explanation for the inhomogeneous broadening at present, bundle effect[10], stress[19], and adsorption of molecules[20] may be responsible.

III.   RESULTS AND DISCUSSION

The PL map of the air-suspended SWNTs is shown in Fig. 2(a). We can find 20 peaks in this energy range. The peak positions were carefully determined from each spectrum. The numerical data are listed in Table I with comparisons to Weisman's data for SDS-wrapped SWNTs[2] and Lefebvre's data for air-suspended SWNTs[15]. The energy differences between the present data and Lefebvre's data are less than 10 meV, except for E_{22} of (13,3). The peak they assigned to (13,3) has been determined as (14,1) in the present work. In the figure, the peak positions are shown by closed circles and squares, which represent type-I and type-II SWNTs, respectively. The data for the SDS-wrapped SWNTs[2] are represented by open circles and squares. The energy differences between the air-suspended and the SDS-wrapped SWNTs are not constant for each (n,m), as shown by the vectors. Detailed data of the peak positions are shown in Fig. 2(b) with the corresponding (n,m). The broken line indicates a boundary between type-I and type-II SWNTs. In the case of the near armchair SNWTs (found near the broken line), both the E_{11} and E_{22} blueshifted. With increasing $n - m$, that is, with decreasing chiral angle, the behavior of the vectors is different between the type-I and type-II SWNTs. In other words, the vectors representing energy shifts have the tendency of rotating counterclockwise for type-I SWNTs and clockwise for type-II SWNTs as $n - m$ increases. This result obviously indicates that the environmental effect on the optical transition energies of SWNTs depends on the (n,m).

The chiral vector (n,m) is a structural parameter which determines the diameter, $d_t = a_{C-C}\sqrt{3(n^2 + nm + m^2)}/\pi$, and chiral angle, $\theta = \tan^{-1}[\sqrt{3}m/(2n + m)]$ of the SWNT. Here, a_{C-C} is the distance between carbon atoms. The energy differences between the air-suspended and the SDS-wrapped SWNTs, $\Delta E_{ii} = E_{ii}^{\mathrm{Air}} - E_{ii}^{\mathrm{SDS}}$, have been investigated with respect to d_t and θ, respectively. Figure 3 shows the ΔE_{11} and ΔE_{22} versus $1/d_t$. The solid lines connect SWNTs belonging to the same $2n + m = $ constant family. Even though the d_t dependence was not clear in the d_t range from 1.0 to 1.3 nm, the family pattern of $2n + m = $ constant was observed. Family patterns observed in usual E_{ii}-$1/d_t$ plots arise from the bandgap modulation due to the trigonal warping effect and the curvature effect which depend on $n - m$[21]. In contrast, in the case of the present ΔE_{ii}-$1/d_t$ plots, the family pattern arises from the (n,m) dependence of the Coulomb interactions between carriers, which also depends on the dielectric constant of the environment as will be described later.

4

In contrast to the d_t dependence, the ΔE_{11} and ΔE_{22} demonstrate the obvious θ dependences as shown in Fig. 4. The θ dependences of ΔE_{11} and ΔE_{22} are different between the type-I and the type-II. In the case of type-I SWNTs, ΔE_{11} increases while ΔE_{22} decreases with increasing θ. Type-II SWNTs show the opposite dependences, such that ΔE_{11} decreases and ΔE_{22} increases with increasing θ. The difference between the type-I and the type-II SWNTs disappears for the SWNTs with θ near 30° (near armchair), and ΔE_{11} and ΔE_{22} approach $\sim$18 and $\sim$14 meV, respectively.

The exciton binding energy in SWNTs is scaled by *intrinsic* parameters such as the diameter and effective mass and by the *extrinsic* environmental dielectric constant[12,13,17]. Here, the effective mass strongly depends on θ due to the trigonal warping effect. The θ determines the angle of the cutting lines with respect to the trigonally-distorted equienergy contours. In the case of near armchair SWNTs, the cutting lines are almost parallel to an edge (K-M) of the hexagonal 2D Brillouin zone. There is little difference in the electronic $E(k)$ dispersion between the type-I and type-II SWNTs, resulting in the same effective mass. In zigzag SWNTs, the difference between type-I and type-II SWNTs is a maximum. The cutting lines perpendicular to a K-M edge (the first conduction band for type-II and the second conduction band for type-I) produce a sharper $E(k)$ dispersion than the cutting line perpendicular to the K-Γ edge (the first conduction band for type-I and the second conduction band for type-II). The ΔE_{11} and ΔE_{22} are plotted in Fig. 5 as a function of effective mass and denoted m_1 and m_2, respectively. Here, we used the effective masses reported by Jorio *et al.*[22], which were calculated by differentiating the $E(k)$ energy dispersion relation obtained by the extended tight binding model at the van Hove singularities. Both ΔE_{11} and ΔE_{22} have a tendency to be smaller for the larger effective mass. This suggests that the (n,m)-dependent environmental effect can be explained by the difference in the effective mass.

The E_{11} and E_{22} mostly blueshifted by a few tens of meV. Although the blueshifts are basically consistent with Lefebvre's report[15], we have found that E_{22} shows redshift at $m_2 > 0.18$; type-II SWNTs with a small θ (near zigzag). When the environmental dielectric constant decreases, the Coulomb interaction is enhanced and the exciton binding energy increases. This leads to a redshift of the optical transition energy in the SWNT. However, the air-suspended SWNTs, where the environmental dielectric constant is smaller than that of SDS-wrapped SWNTs, mostly showed blueshifts as compared to the SDS-

wrapped SWNTs as described above. The optical transition energy in SWNTs is given by a summation of the bandgap and the exciton binding energy. It should be noted that the bandgap is perturbed by the electron-electron interaction, and, consequently the change in the environmental dielectric constant affects not only the exciton binding energy, but also the bandgap[12]. The observed blueshifts are thought to be due to the increase in the repulsion energy of the electron-electron interaction with the decrease in the dielectric constant.

As reported by Ando[12] and also by Spataru *et al.*[23], the electron-electron repulsion energy is larger in magnitude than the exciton binding energy. Therefore, if we consider the both energies show similar dependence on the dielectric constant, the increase in the electron-electron repulsion energy exceeds the increase in the exciton binding energy when the dielectric constant decreases. This results in the blueshift of optical transition energies.

On the other hand, in the SWNTs with m_2 larger than 0.18, the E_{22} showed a redshift as shown in Fig. 5 The energy shift would be determined by a competition between the electron-electron repulsion energy and the exciton binding energy. It is inferred from the redshift that the exciton binding energy is larger than the electron-electron repulsion energy in the E_{22} level of these SWNTs. To our knowledge, there are no theoretical reports about (n,m) or effective mass dependence of electron-electron repulsion energy, whereas the dependence of exciton binding energy has been reported by Perebeinos et al.[13] To clarify the origin of the redshift, a systematic study is necessary.

IV. CONCLUSION

In summary, we have investigated the environmental effect on photoluminescence of SWNTs by comparing PL maps between air-suspended and SDS-wrapped SWNTs. The E_{11} and E_{22} of the air-suspended SWNTs mostly showed blueshifts, as compared to the SDS-wrapped SWNTs. An exception to this was seen in the E_{22} of the near-zigzag type-II SWNTs, which showed redshifts. The blueshifts are understood as an increase in the repulsion energy of an electron-electron interaction due to the reduction of the dielectric constant outside the SWNT. ΔE_{11} and ΔE_{22} showed obvious chiral angle dependences. With increasing chiral angle, ΔE_{11} increased in type-I SWNTs and decreased in type-II SWNTs: ΔE_{22} showed the opposite dependences. The (n,m) dependence of the environmental effect can be explained by the (n,m) dependence of the effective mass. Recent report by Finnie

et al. describes that the band-gap transition in the PL which depends on the temperature and environmental atmosphere[19]. They have suggested that the adsorption and desorption of molecules such as oxygen and water are responsible for the band-gap transition. Further research is necessary to understand the effects of the environment with regard to the atmosphere as well as the dielectric constant on the optical transition energies in SWNTs.

---

* Also at PRESTO, Japan Science and Technology Agency, 4-1-8 Honcho, Kawaguchi, Saitama 332-0012, Japan; Electronic address: `yohno@nuee.nagoya-u.ac.jp`

† Also at Institute for Advanced Research, Nagoya University, Furo-cho, Chikusa-ku, Nagoya, 464-8601, Japan

[1] S. M. Bachilo, M. S. Strano, C. Kittrell, R. H. Hauge, R. E. Smalley, and R. B. Weisman, Science **298**, 2361 (2002).

[2] R. B. Weisman and S. M. Bachilo, Nano Lett. **3**, 1235 (2003).

[3] Y. Miyauchi, S. Chiashi, Y. Murakami, Y. Hayashida, S. Maruyama, Chem. Phys. Lett. **387**, 198 (2004).

[4] H. Htoon, M. J. O'Connell, P. J. Cox, S. K. Doorn, and V. I. Klimov, Phys. Rev. Lett. **93**, 027401 (2004).

[5] D. A. Tsyboulski, S. M. Bachilo, and R. B. Weisman, Nano Lett. **5**, 975 (2005).

[6] S. G. Chou, H. B. Ribeiro, E. B. Barros, A. P. Santos, D. Nezich, Ge. G. Samsonidze, C. Fantini, M. A. Pimenta, A. Jorio, F. Plentz Filho, M. S. Dresselhaus, G. Fresselhaus, R. Saito, M. Zheng, G. B. Onoa, E. D. Semke, A. K. Swan, M. S. Ünlü, and B. B. Goldberg, Chem. Phys. Lett. **397**, 296 (2004).

[7] F. Wang, G. Dukovic, L. E. Brus, T. F. Heinz, Science **308**, 838 (2005).

[8] M. J. O'Connell, S. M. Bachilo, C. B. Huffman, V. C. Moore, M. S. Strano, E. H. Haroz, K. L. Rialon, P. J. Boul, W. H. Noon, C. Kittrell, J. Ma, R. H. Hauge, R. B. Weisman, and R. E. Smalley, Science **297**, 593 (2002).

[9] T. Hertel, A. Hagen, V. Talalaev, K. Arnold, F. Hennrich, M. Kappes, S. Rosenthal, J. McBride, H. Ulbricht, and E. Flahaut, Nano Lett. **5**, 511 (2005).

[10] C. Fantini, A. Jorio, M. Souza, M. S. Strano, M. S. Dresselhaus, and M. A. Pimenta, Phys. Rev. Lett. **93**, 147406 (2004).

[11] V. C. Moore, M. S. Strano, E. H. Haroz, R. H. Hauge, R. E. Smalley, J. Schmidt, and Y. Talmon, Nano Lett. **3**, 1379 (2003).

[12] T. Ando J. Phys. Soc. Japan **74**, 777 (2005).

[13] V. Perebeinos, J. Tersoff, and Ph. Avouris, Phys. Rev. Lett. **92**, 257402 (2004).

[14] J. Lefebvre, Y. Homma, and P. Finnie, Phys. Rev. Lett. **90**, 217401 (2003).

[15] J. Lefebvre, J. M. Fraser, Y. Homma, and P. Finnie, Appl. Phys. A **78**, 1107 (2004).

[16] Y. Ohno, S. Kishimoto, and T. Mizutani, Nanotechnology **17**, 549 (2006).

[17] T. G. Pedersen, Carbon **42**, 1007 (2004).

[18] Y. Marukami, Y. Miyauchi, S. Chiashi, and S. Maruyama, Chem. Phys. Lett. **374**, 53 (2003).

[19] K. Arnold,S. Lebedkin, O. Kiowski, F. Hennrich, and M. M. Kappes, Nano Lett. **4**, 2349 (2004).

[20] P. Finnie, Y. Homma, and J. Lefebvre, Phys. Rev. Lett. **94**, 247401 (2005).

[21] G. G. Samsonidze, R. Saito, N. Kobayashi, A. Grüneis, J. Jiang, A. Jorio, S. G. Chou, G. Dresselhaus, and M. S. Dresselhaus, Appl. Phys. Lett. **85**, 5703 (2004).

[22] A. Jorio, C. Fantini, M. A. Pimenta, R. B. Capaz, G. G. Samsonidze, G. Dresselhaus, M. S. Dresselhaus, J. Jian, N. Koabayashi, A. Grüneis, and R. Saito, Phys. Rev. B **71**, 075401 (2005).

[23] C. D. Spataru, S. Ismail-Beigi, L. X. Benedict, and S. G. Louie, Phys. Rev. Lett. **92**, 077402 (2004).

TABLE I: Experimental transition energies of air-suspended SWNTs compared to Weisman's data for SDS-wrapped SNWTs[2] and Lefebvre's data for air-suspended SWNTs[15]. The energy differences between the air-suspended and the SDS-wrapped SWNTs, $\Delta E_{ii} = E_{ii}^{\mathrm{Air}} - E_{ii}^{\mathrm{SDS}}$, are also listed.

| (n,m) | $2n+3$, | air-suspended | | | | SDS-wraped[2] | | air-suspended[15] | |
	Type-I/II	E_{11}	ΔE_{11}	E_{22}	ΔE_{22}	E_{11}	E_{22}	E_{11}	E_{22}
		(eV)	(meV)	(eV)	(meV)	(eV)	(eV)	(eV)	(eV)
(8,7)	23, II	1.003	+22	1.716	+14	0.981	1.702	-	-
(9,8)	23, II	0.898	+19	1.545	+12	0.879	1.533	0.904	1.550
(10,5)	25, I	1.010	+17	1.597	+23	0.993	1.574	1.011	1.601
(11,3)	25, I	1.051	+15	1.588	+24	1.036	1.564	1.060	1.593
(12,1)	25, I	1.073	+13	1.586	+34	1.060	1.552	-	-
(9,7)	25, I	0.959	+21	1.580	+17	0.938	1.563	0.964	1.588
(10,6)	26, II	0.923	+23	1.646	+2	0.900	1.644	0.929	1.651
(10,8)	28, I	0.861	+17	1.441	+15	0.844	1.426	-	-
(11,6)	28, I	0.901	+14	1.461	+15	0.887	1.446	-	-
(12,4)	28, I	0.939	+15	1.460	+10	0.924	1.450	-	-
(13,2)	28, I	0.963	+14	1.468	+22	0.949	1.446	-	-
(14,0)	28, I	0.966	+9	1.468	+25	0.957	1.443	-	-
(10,9)	29, II	0.812	+15	1.414	+19	0.797	1.395	-	-
(11,7)	29, II	0.839	+21	1.486	+2	0.818	1.484	-	-
(12,5)	29, II	0.854	+27	1.562	-1	0.827	1.563	0.860	1.566
(13,3)	29, II	0.857	+29	1.614	-10	0.828	1.624	0.865	1.640
(14,1)	29, II	0.856	+30	1.641	-16	0.826	1.657	-	-
(13,6)	32, II	0.778	+18	1.421	+2	0.760	1.419	-	-
(14,4)	32, II	0.785	+21	1.469	-3	0.764	1.472	-	-
(15,2)	32, II	0.792	+28	1.505	-3	0.764	1.508	-	-
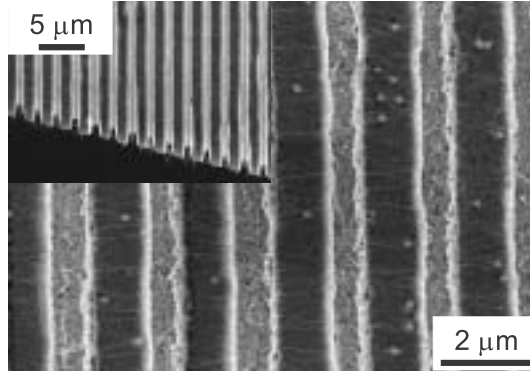
FIG. 1: Plan-view and bird-view (inset) SEM images of air-suspended SWNTs grown on a grated quartz substrate. Both the period and depth of a groove are 2 μm. The SWNTs bridged in the groove during growth and aligned perpendicular to the groove.
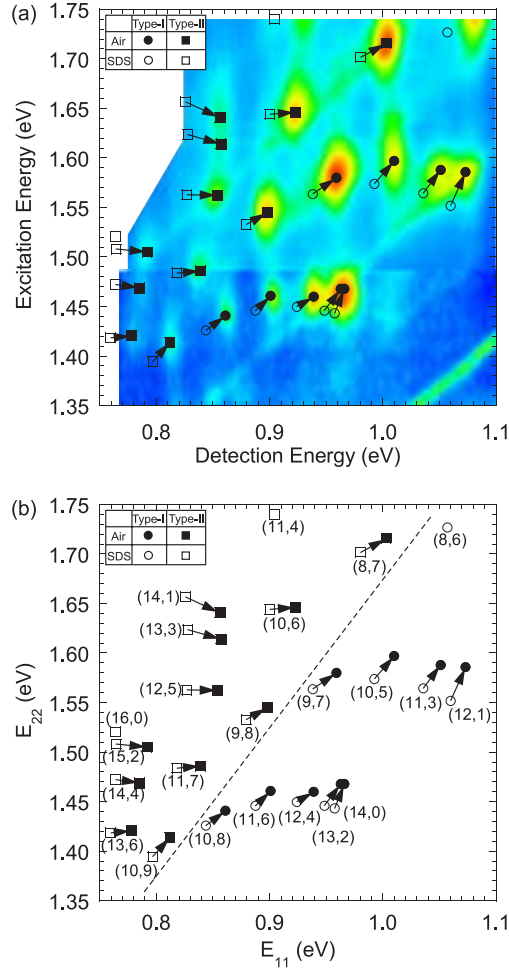
FIG. 2: (a) PL map of air-suspended SWNTs, and (b) E_{11} and E_{22} of air-suspended SWNTs, compared to those of SDS-wrapped SWNTs reported by Weisman *et al*[2]. Here, the closed squares and circles represent the air-suspended SWNTs, and the open squares and circles represent the SDS-wrapped SWNTs. The circles are type-I $[(2n + m) \bmod 3 = 1]$ SWNTs, and squares are type-II $[(2n + m) \bmod 3 = 2]$ SWNTs. Vectors indicate the energy shifts of E_{11} and E_{22} of the air-suspended SWNTs from those of SDS-wrapped SWNTs, ΔE_{11} and ΔE_{22}. The broken line in (b) indicates a boundary between type-I and type-II.
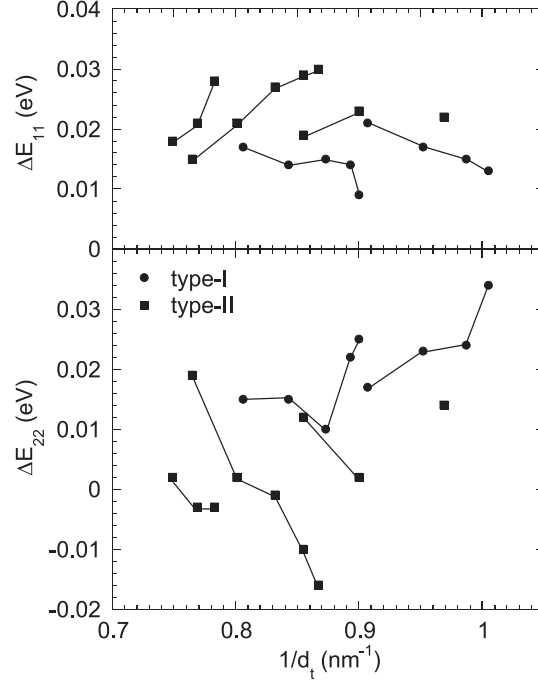
FIG. 3: ΔE_{11} and ΔE_{22} as a function of $1/d_t$. The circles and squares represent type-I and type-II, respectively. The solid lines connect SWNTs belonging to the same $2n + m = $ constant family.
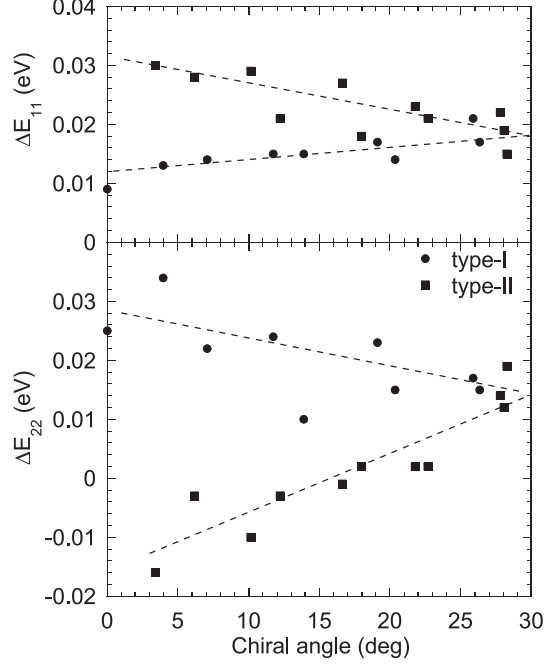
FIG. 4: ΔE_{11} and ΔE_{22} as a function of θ. The circles and squares represent type-I and type-II, respectively. The ΔE_{11} and ΔE_{22} show the obvious θ dependences. ΔE_{11} decreases in type-I SWNTs and increases in type-II SWNTs with an increase in θ. ΔE_{22} shows the opposite dependences. The difference between the type-I and the type-II SWNTs disappears for the near-armchair SWNTs ($\theta \sim 30°$).
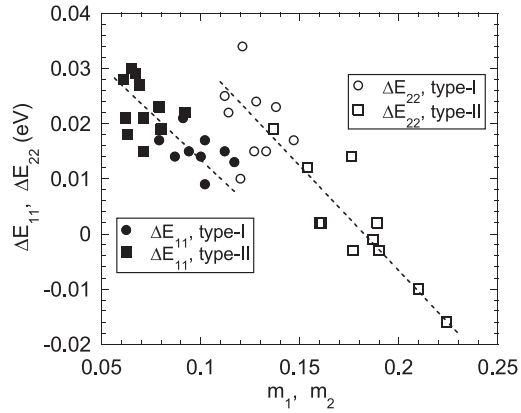

FIG. 5: ΔE_{11}-m_1 and ΔE_{22}-m_2 plots. The circles and squares represent type-I and type-II, respectively. The ΔE_{11} and ΔE_{22} are smaller for the larger effective mass.